

## **CHRNA5 links chandelier cells to protection against amyloid pathology in human aging and Alzheimer's Disease**

Jonas Rybnicek<sup>1</sup>, Yuxiao Chen<sup>2</sup>, Milos Millic<sup>2</sup>, JoAnne McLaurin<sup>3</sup>, Philip L De Jager<sup>4</sup>, Julie A Schneider<sup>5</sup>, Yanling Wang<sup>6</sup>, David A Bennett<sup>6</sup>, **Shreejoy Tripathy**\*<sup>1, 2, 7, 8</sup>, **Daniel Felsky**\*<sup>2, 7, 8</sup>, **Evelyn K Lambe**\*<sup>1, 7, 9</sup>

1. Department of Physiology, University of Toronto, Toronto ON, Canada
2. Krembil Centre for Neuroinformatics, Centre for Addiction and Mental Health, Toronto ON, Canada
3. Biological Sciences, Sunnybrook Research Institute, Toronto, ON M4N 3M5, Canada.
4. Center for Translational & Computational Neuroimmunology, Department of Neurology and the Taub Institute for Research on Alzheimer's Disease and the Aging Brain, Columbia University Irving Medical Center, New York NY, USA
5. Department of Pathology, Rush University, Chicago IL, USA
6. Department of Neurological Sciences, Rush University, Chicago IL, USA
7. Department of Psychiatry, University of Toronto, Toronto ON, Canada
8. Institute of Medical Science, University of Toronto, Toronto ON, Canada
9. Department of OBGYN, University of Toronto, Toronto ON, Canada

\*Co-corresponding authors

**Co-Corresponding Authors email addresses:**

**Shreejoy Tripathy:** [shreejoy.tripathy@camh.ca](mailto:shreejoy.tripathy@camh.ca)

**Dan Felsky:** [daniel.felsky@camh.ca](mailto:daniel.felsky@camh.ca)

**Evelyn Lambe:** [evelyn.lambe@utoronto.ca](mailto:evelyn.lambe@utoronto.ca)

**Number of Figures:** 5

**Number of Tables:** 1

**Word count:** Abstract: 216, Introduction: 541, Discussion: 1120

**Conflicts of Interest:** None

**Acknowledgements:** This work was supported by the Canadian Institutes of Health Research (CIHR; EKL; PJT-153101, MOP89825; EKL; NGN-171423, ST; 428404, DF), Krembil Foundation (DF, ST), Koerner Family Foundation (DF), CAMH Discovery Fund (DF, ST), Kavli Foundation (ST), McLaughlin Foundation (ST), Natural Sciences and Engineering Research Council of Canada (RGPIN-2020-05834 and DGEGR-2020-00048; ST). JM is supported by the Canadian Research Chairs program, as a Tier 1 Chair. ROSMAP is supported by P30AG10161, P30AG72975, R01AG15819, R01AG17917, U01AG46152, U01AG61356. ROSMAP resources can be requested at <https://www.radc.rush.edu>

1 **Abstract**

2 Changes in high-affinity nicotinic acetylcholine receptors are intricately connected to neuropathology in  
3 Alzheimer's Disease (AD). Protective and cognitive-enhancing roles for the nicotinic  $\alpha 5$  subunit have  
4 been identified, but this gene has not been closely examined in the context of human aging and  
5 dementia. Therefore, we investigate the nicotinic  $\alpha 5$  gene *CHRNA5* and the impact of relevant single  
6 nucleotide polymorphisms (SNPs) in prefrontal cortex from 922 individuals with matched genotypic  
7 and *post-mortem* RNA sequencing in the Religious Orders Study and Memory and Aging Project  
8 (ROS/MAP). We find that a genotype robustly linked to expression of *CHRNA5* (rs1979905A2) predicts  
9 significantly reduced cortical  $\beta$ -amyloid load. Yet, co-expression analysis shows a clear dissociation  
10 between expression of *CHRNA5* and other cholinergic genes, suggesting a distinct cellular expression  
11 profile for the human nicotinic  $\alpha 5$  subunit. Consistent with this prediction, single nucleus RNA  
12 sequencing from 22 individuals reveals disproportionately-elevated *CHRNA5* expression in chandelier  
13 cells. These interneurons are enriched in amyloid-binding proteins and also play a vital role in  
14 excitatory/inhibitory (E/I) balance. Cell-type proportion analysis from 549 individuals demonstrates  
15 chandelier cells have increased amyloid vulnerability in individuals homozygous for the missense  
16 *CHRNA5* SNP (rs16969968A2) that impairs function/trafficking of nicotinic  $\alpha 5$ -containing receptors.  
17 These findings suggest that *CHRNA5* and its nicotinic  $\alpha 5$  subunit exert a neuroprotective role in aging and  
18 Alzheimer's disease potentially centered on chandelier interneurons.

19  
20 **Keywords:** Alzheimer's disease, prefrontal cortex, acetylcholine, nicotinic receptors, chandelier cells,  
21 interneurons, amyloid, attention

22

23

24

25

26

27

28

29

30

31

## 32 Introduction

33 The cholinergic system plays a critical role in the pathology of Alzheimer's disease (AD) (1), a  
34 neurodegenerative disease marked by the accumulation of  $\beta$ -amyloid peptide ( $\beta$ -amyloid) and  
35 neurofibrillary tangles of phosphorylated tau in the brain (2). In AD, there are well-characterized  
36 disturbances in the excitation/inhibition (E/I) balance in cerebral cortex (3,4) arising from the disruption  
37 of inhibitory signalling. The shift toward higher excitation in the cortex is associated with cognitive  
38 impairment in AD.

39 The cholinergic system is an important regulator of E/I balance in the prefrontal cortex (PFC) (5,6) and is  
40 central to one of the first mechanistic explanations of cognitive deficits in AD; the so-called *cholinergic*  
41 *hypothesis* (7). In AD, there is a decrease of cortical nicotinic acetylcholine receptor binding (8,9), and  $\beta$ -  
42 amyloid binding to nicotinic receptors has been postulated as a potential mediator of AD pathology  
43 (10,11) possibly via blockade of these receptors (12,13). By contrast, stimulation of neuronal nicotinic  
44 receptors has been found to improve neuron survival in AD pathology (14), promote neurogenesis, and  
45 improve cognition (15,16). Promoting nicotinic signalling using acetylcholinesterase inhibitors is one of  
46 the mainstay AD treatments (17).

47 High-affinity nicotinic acetylcholine receptors are hetero-pentamer cation channels most commonly  
48 composed of  $\alpha 4$  and  $\beta 2$  subunits ( $\alpha 4\beta 2$ ) (18). Deep layer PFC pyramidal cells express nicotinic receptors  
49 also containing the auxiliary  $\alpha 5$  subunit (18,19). Nicotinic  $\alpha 5$  subunits do not contribute to the  
50 acetylcholine binding site and cannot form functional receptors on their own (19), requiring the binding  
51 sites provided by partner subunits  $\alpha 4$  and  $\beta 2$ , and forming the  $\alpha 4\beta 2\alpha 5$  nicotinic receptor. The  $\alpha 5$  subunit  
52 alters the kinetics of nicotinic receptors (20) and increases their permeability to calcium ions (21,22).  
53 Importantly,  $\beta$ -amyloid binds less readily to  $\alpha 4\beta 2\alpha 5$  than  $\alpha 4\beta 2$  nicotinic receptors (12), which raises the  
54 question of a possible protective role of the  $\alpha 5$  subunit in AD pathology.

55 The nicotinic  $\alpha 5$  subunit has previously been linked to cognitive performance, with loss or disruption of  
56 this subunit impairing performance in attentional tasks in rodents (23,24). In humans, single nucleotide  
57 polymorphisms (SNPs) affecting the expression and function/trafficking of the *CHRNA5* gene, which  
58 codes for the  $\alpha 5$  subunit, have been linked to attentional and cognitive deficits (25,26). These SNPs are  
59 also linked to smoking (27), a major AD risk factor (28). However, the role of *CHRNA5* in aging and AD is  
60 unknown.

61 To address this critical gap, we built a multi-step model of the connections between SNPs affecting the  
62 expression and function of *CHRNA5*, and age-related cognitive and neuropathological phenotypes using  
63 detailed clinical and post-mortem data from the Religious Order Study and Memory and Aging Project  
64 (ROS/MAP) (29). Next, we leveraged single-nucleus RNAseq to determine the cell-type expression  
65 pattern of *CHRNA5* in the PFC. We then used a gene ontology analysis of cortical patch-seq data (30) to  
66 elucidate the functional makeup of the cell type with the highest *CHRNA5* levels in the PFC, the  
67 chandelier cells. Finally, we probed an estimated cell type proportion dataset from the PFC (31) to assess  
68 the interaction effect of *CHRNA5* SNPs and Alzheimer's disease pathology on this *CHRNA5*-enriched cell  
69 type. The results of our study suggest a novel role for *CHRNA5* in maintaining the E/I balance in the  
70 forebrain and as a potential new target for therapies aiming to promote neuronal survival in AD.

71

72

73

## 74 **Methods**

### 75 **Study cohort**

76 We accessed data from 2004 deceased individuals from the ROS/MAP cohort study (29), of whom 1732  
77 were autopsied. Both studies enrolled individuals without known dementia. ROS enrolls elderly nuns,  
78 priests, and members of clergy, whereas MAP enrolls individuals from community facilities and individual  
79 homes. Both studies were approved by an Institutional Review Board of Rush University Medical Centre.  
80 Participants gave informed consent for annual clinical evaluation, completed a repository consent  
81 allowing their resources to be shared, and signed an Anatomic Gift Act for brain donation at the time of  
82 death. Most individuals assessed were female (68%). The average age at study entry was  $80.5 \pm 0.16$   
83 years and the average age at death was  $89.2 \pm 0.2$  years. All data was retrieved from the Synapse AMP-  
84 AD Knowledge Portal (Synapse ID: syn2580853).

### 85 **Selection of candidate single nucleotide polymorphisms (SNPs)**

86 Nicotinic  $\alpha 5$  subunits (encoded by *CHRNA5*) do not contribute to the acetylcholine binding site and  
87 cannot form functional receptors on their own (19). In prefrontal cortex, the nicotinic  $\alpha 5$  subunits  
88 participate in pentameric receptors with two binding sites contributed by partner subunits:  $\alpha 4$  (encoded  
89 by *CHRNA4*) and  $\beta 2$  (encoded by *CHRNA2*) (18). Together, these subunits form  $\alpha 4\beta 2\alpha 5$  nicotinic  
90 receptors. While the current focus is *CHRNA5*, we also probed the impact of polymorphisms relevant to  
91 its receptor partners *CHRNA4* or *CHRNA2* for perspective. The specific polymorphisms were selected  
92 based on their reported effects on expression, coding, or clinical response. (*CHRNA5*:(27,32,33);  
93 *CHRNA2*: (34,35);; *CHRNA4*: (36).

### 94 **Genotype data preparation and imputation, quality control, generation of bulk gene expression 95 residuals**

96 Details on the ROS/MAP cohort genotyping and handling of the post-mortem samples have been  
97 previously published (37) and are described briefly together with the quality control approaches and  
98 generation of the gene expression residuals in **Supplemental Methods**.

### 99 **Neuropathology and cognitive scores**

100 A detailed description of the neuropathology and cognitive variables in ROSMAP is included in  
101 **Supplemental Methods** and on the RADC Research Resource Sharing Hub.

### 102 **Single-nucleus RNA sequencing data processing**

103 The single-nucleus gene counts and metadata available from Cain et al. 2020 (31) on synapse (ID:  
104 syn16780177) were converted into a Seurat object (38) in R Studio for further processing. Potential  
105 doublets were removed by filtering out cells with over 2500 detected features, and potential dead or  
106 dying cells were removed by excluding cells expressing over 5% mitochondrial genes. Cell type  
107 annotations were indicated in the data as described in the metadata downloaded from the Cain et al.  
108 2020 Synapse repository (ID: syn16780177). The snRNAseq data was log-normalized and matched with  
109 genotype data ( $n = 22$  individuals). *CHRNA5* expression was averaged per cell type per individual and  
110 *CHRNA5* levels in different cell types were then compared between cell types by one-way ANOVA with  
111 Tukey's post-hoc t-test. To prevent bias for rare cell types in calculating average *CHRNA5* expression per  
112 cell type per individual, cell types with fewer than 100 individual cells represented in the original data

113 (not aggregated) were removed (the layer 5 FEZF2 ET cell type was excluded from analysis as only 93  
114 cells of this type were present in the genotype-matched snRNAseq dataset).

### 115 **Gene ontology of chandelier cell genes**

116 A set of genes which are upregulated in PVALB+ chandelier cells versus PVALB+ chandelier cells was  
117 previously generated by Bakken and colleagues (30). From this list we first excluded all genes not  
118 specifically upregulated in humans (final n = 222) To determine the ontology of this gene set we used the  
119 Gene Ontology Resource ([geneontology.org](http://geneontology.org)), searching specifically for molecular function.

### 120 **Estimates of relative cell type proportions from bulk DLPFC RNAseq**

121 Estimates of cell-type proportions from bulk DLPFC RNAseq data from 640 ROS/MAP participants was  
122 performed and described by Cain et al. 2020 (31). In brief: The authors developed a custom regression-  
123 based consensus model, CelMod, to extract cell cluster specific genes from the snRNAseq dataset from  
124 24 ROS/MAP participants, and then used these genes to estimate the proportions of different cell  
125 subtypes in the bulk DLPFC RNAseq dataset from 640 ROS/MAP individuals. The deconvolved cell-type  
126 proportion data from the DLPFC was available on request from the research group (Cain et al. 2020  
127 personal communication). We matched the cell type proportion data with genotype, bulk DLPFC RNAseq,  
128 and neuropathology (brain levels of  $\beta$ -amyloid and tau) data (final n = 549 individuals). At the time of  
129 analysis full cell-type annotations (like that in the snRNAseq data) were only available for the different  
130 classes of inhibitory neuron proportions. The estimated proportions of a GABAergic neuron subtype  
131 defined by its expression of the marker gene combination PVALB+/LHX6+/THSD7A+, were determined  
132 (Cain et al. 2020 personal communication) to represent chandelier cell proportions in DLPFC. Observed  
133 differences in the estimated proportions of this cell subtype represent a difference in the proportion of  
134 this cell subtype in the broad cell class (GABAergic neurons). Further information on the cell type  
135 proportions is provided in **Supplemental Methods**.

### 136 **Statistical approaches**

137 A detailed description of the statistical analyses is provided in **Supplemental Methods**.

## 138 **Results**

### 139 **Expression of $\alpha 4\beta 2\alpha 5$ receptor component genes is affected by single nucleotide polymorphisms**

140 To identify effects in aging and dementia of gene variants previously shown in younger adults to  
141 influence *CHRNA5* expression (33) and  $\alpha 5$  coding (21,39), we examined brain expression quantitative  
142 trait loci (eQTL). The variants were in weak-moderate linkage disequilibrium in our European ancestry  
143 sample ( $r^2=0.34$ ), in agreement with previous work (33). We also found that dosage of the A allele of the  
144 missense SNP rs16969968 (minor allele frequency (MAF) = 0.33) in the coding region of *CHRNA5* (**Fig 1B**)  
145 was associated with lower *CHRNA5* expression ( $t = -13.93$   $p = 3.98 \times 10^{-40}$ ), consistent with existing data  
146 (40). A different SNP haplotype in the regulatory region upstream of *CHRNA5* (**Fig 1B**), denoted here by  
147 the A allele of the tag SNP rs1979905 (MAF = 0.43), was associated with higher *CHRNA5* expression ( $t =$   
148  $27.87$ ,  $p = 5.94 \times 10^{-124}$ ) (**Fig. 1C**). Furthermore, analyses of the coding-SNP rs16969968 and the regulatory-  
149 SNP rs1979905 together (**Fig. 1D**) showed that *CHRNA5* expression is predominantly regulated by the  
150 regulatory-SNP rs1979905 rather than the coding-SNP, rs16969968, as all rs1979905 A allele non-carriers  
151 showed similar levels of *CHRNA5* mRNA regardless of the rs16969968 A allele (Nested one-way ANOVA:  
152  $F(2) = 229.6$ ; Šidák's post-hoc test for multiple comparisons: rs1979905 A1 vs. A0  $p = 8 \times 10^{-6}$ , A2 vs. A1  $p =$   
153  $0.004$ , A2 vs A0  $p = 4 \times 10^{-6}$ ). This was also demonstrated using a conditional eQTL model, where the effect

154 of rs16969968 A allele on *CHRNA5* expression was lost when co-varying for rs1979905 A allele  
155 (rs16969968A:  $t = -1.068$ ,  $p = 0.2815$ ; rs1979905A:  $t = 21.931$ ,  $p = 6.140 \times 10^{-86}$ ). No association between  
156 *CHRNA5* expression and disease state was detected (**Supplemental Fig. S1**). No trans-eQTL effects were  
157 detected (**Fig. 1E**) between either of these SNPs and the expression of required partner nicotinic subunit  
158 genes, *CHRNA4* and *CHRN2*.

159 To assess the  $\alpha 4$  and  $\beta 2$  nicotinic subunits required for the formation of  $\alpha 5$ -containing  $\alpha 4\beta 2\alpha 5$   
160 receptors, we extended our eQTL analyses to SNPs in *CHRNA4* and *CHRN2*, focusing on those associated  
161 with altered gene expression or clinical effects(35,36,41). Without exception, eQTL SNP effects for these  
162 genes were weaker than those of rs16969968 and rs1979905 for *CHRNA5*: the T allele of *CHRN2*  
163 intronic variant rs2072660 (MAF = 0.23) was associated with lower *CHRN2* expression ( $t = -5$ ,  $p =$   
164  $7.05 \times 10^{-7}$ ), and a similar association with *CHRN2* expression was seen with the T allele of the *CHRN2*  
165 non-coding variant rs4292956 (MAF = 0.07) ( $t = -5.244$ ,  $p = 2.02 \times 10^{-7}$ ) (**Fig. 1E**). For *CHRNA4*, the G allele  
166 of missense variant rs1044396 (MAF = 0.45) in the coding region of *CHRNA4* was associated with higher  
167 *CHRNA4* expression ( $t = 3.67$ ,  $p = 0.0003$ ). We also used the Gene Query function of the xQTLserve online  
168 tool (DLPFC of 534 ROS/MAP participants) to identify the T allele of the intronic variant rs45497800 as  
169 associated with decreased *CHRNA4* expression ( $t = -6.92$ ,  $p = 1.32 \times 10^{-11}$ ). We then replicated this  
170 association in our larger cohort of 924 ROS/MAP individuals (MAF = 0.07) ( $t = -4.57$ ,  $p = 5.54 \times 10^{-6}$ ) (**Fig.**  
171 **1E**). No associations were found between these SNPs and the expression of other high-affinity nicotinic  
172 receptor subunit genes (**Fig. 1E**).

### 173 ***CHRNA5* polymorphisms are not associated with smoking status in this largely non-smoking population**

174 The percentage of participants identified as never, previous, and current smokers (**Supplemental**  
175 **Methods**) was 68.2, 29.4, and 2.4 respectively. To investigate previously-reported (25,42) associations  
176 between genotype for the *CHRNA5* SNPs and smoking status at baseline (current/former/never smoked),  
177 we used a Chi-squared test and found no relationship (rs1979905\_A :  $\chi^2(4) = 1.575$ ,  $p = 0.813$ ;  
178 rs16969968\_A:  $\chi^2(4) = 1.317$ ,  $p = 0.858$ ) in this largely non-smoking population. Smoking status was not  
179 used in further analysis, unless specifically indicated.

### 180 **A *CHRNA5* polymorphism is negatively associated with brain $\beta$ -amyloid levels**

181 To address interrelationships among nicotinic subunit expression, nicotinic SNPs, and neuropathological  
182 and cognitive phenotypes, we used clinical and post-mortem data in a multi-step model, the inclusion  
183 and exclusion criteria for this model can be found in **Supplemental Fig. S2**. As illustrated in **Fig. 1F**, both  
184  $\beta$ -amyloid and tau pathology were negatively associated with global cognitive performance proximal to  
185 death (tau:  $t = -18.87$ ,  $p = 5.77 \times 10^{-70}$ ; amyloid:  $t = -7.88$ ,  $p = -6.99 \times 10^{-15}$ ) and positively associated with  
186 each other ( $t = 12.59$ ,  $p = 2.14 \times 10^{-34}$ ). Of the SNPs examined, only the SNP increasing *CHRNA5* expression  
187 had a significant association with AD neuropathology, with the A allele of the regulatory-SNP rs1979905  
188 negatively associated with  $\beta$ -amyloid load ( $t = -2.79$ ,  $p = 0.005$ ). This association remained significant  
189 after false discovery rate (FDR) correction for multiple comparisons ( $p_{FDR} = 0.021$ )(43), *CHRNA5*  
190 expression was associated negatively with  $\beta$ -amyloid load prior to FDR correction ( $t = -2.23$ ,  $p = 0.026$ ).  
191 By contrast, the expression of the major nicotinic subunit genes *CHRNA4* and *CHRN2* showed significant  
192 positive associations with the last global cognition score, which remained significant after FDR correction  
193 (*CHRNA4*:  $t = 2.98$ ,  $p_{FDR} = 0.013$ ; *CHRN2*:  $t = 3.43$ ,  $p_{FDR} = 0.003$ ). Conversely, the rs2072660 T allele,  
194 associated with lower *CHRN2* expression, was negatively associated with the last global cognition score  
195 ( $t = -1.98$ ,  $p = 0.047$ ). A similar negative association with the last global cognition score ( $t = -2.29$ ,  $p =$   
196  $0.021$ ) was found for the T allele of the *CHRN2* SNP rs4292956.

### 197 ***CHRNA5* expression does not tightly correlate with other components of the cholinergic system**

198 To further investigate the interrelationships among *CHRNA5* and the major nicotinic subunits as well as  
199 other components of the cholinergic system, we performed a series of expression correlation analyses.  
200 Most of the major components of the cholinergic system which were detected in bulk DLPFC data of the  
201 ROS/MAP individuals (*CHRNA2*, *CHRNA4*, *CHRNA7*, *CHRN2*, *CHRM3*, *CHRM1* and *ACHE*) showed  
202 significant positive correlation with each other (**Fig. 1G**). By contrast, *CHRNA5* stood out as showing no  
203 positive correlation with any of the other major cholinergic genes and only weak negative correlations  
204 with the expression of *CHRN2* and *CHRM1* (**Table 1**). Considering that the expression of *CHRNA5*,  
205 *CHRN2*, and *CHRNA4* are required for the assembly of the high-affinity  $\alpha 4\beta 2\alpha 5$  nicotinic receptor, it was  
206 surprising to see that *CHRNA5* expression was not positively correlated with either *CHRNA4* or *CHRN2*  
207 (**Fig. 1G** and **Table 1**). Therefore, we next investigated whether this lack of correlation may arise from  
208 differences in the cell-type specific expression of *CHRNA5* compared to the major nicotinic receptor  
209 subunits, *CHRNA4* and *CHRN2*, which are more broadly expressed.

### 210 ***CHRNA5* shows stronger expression in chandelier interneurons than most other cell classes**

211 To assess the cell-type specificity of *CHRNA5* expression in the ROS/MAP cohort, we calculated the  
212 average *CHRNA5* expression per cell type per individual using the genotype-matched single-nucleus  
213 RNAseq data available from the DLPFC in a subset of 22 ROS/MAP participants (31)(2 individuals lacked  
214 genotyping data). In this small dataset, *CHRNA5* was expressed at a low level across a number of  
215 different excitatory, inhibitory, and nonneuronal cell types (**Fig. 2A**), with significantly higher expression  
216 in inhibitory PVALB+ chandelier cells (as identified by Cain et al. 2020). Chandelier cells had significantly-  
217 higher expression of *CHRNA5* compared to most other cell types (One-way ANOVA:  $F(21) = 3.439$ ,  $p =$   
218  $6.1 \times 10^{-7}$ ; Tukey's post-hoc t-test Chandelier cells vs. 18 out of 19 other cell types:  $p < 0.05$ ) (**Fig. 2A**). By  
219 contrast, chandelier cell expression of *CHRNA4* and *CHRN2* were at a similar level in chandelier cells to  
220 their expression levels in many other cell types (**Fig. 2B**).

221 To confirm the novel finding that chandelier cells show stronger *CHRNA5* expression compared to other  
222 classes of neurons, we probed publicly available cell-type specific gene expression databases of human  
223 brain tissue. Using the Allen Institute SMART-seq single-cell transcriptomics data from multiple cortical  
224 areas [https://celltypes.brain-map.org/rnaseq/human\\_ctx\\_smart-seq](https://celltypes.brain-map.org/rnaseq/human_ctx_smart-seq) we found *CHRNA5* expression to be  
225 highest in a PVALB+/SCUBE3+ inhibitory cell type (0.06 trimmed mean *CHRNA5* expression) likely  
226 representing chandelier cells (44), and in a co-clustering PVALB+/MFI+ cell type (0.06 trimmed mean  
227 *CHRNA5* expression). Highest expression of *CHRNA5* in chandelier cells compared to all other cell types is  
228 also replicated in the Seattle Alzheimer's Disease Brain Cell Atlas ([https://knowledge.brain-](https://knowledge.brain-map.org/data/5IU4U8BP711TR6KZ843/2CD0HDC5PS6A58T0P6E/compare?cellType=WholeTaxonomy&geneOption=CHRNA5&metadata=Cognitive%20Status&comparison=dotplot)  
229 [map.org/data/5IU4U8BP711TR6KZ843/2CD0HDC5PS6A58T0P6E/compare?cellType=Whole](https://knowledge.brain-map.org/data/5IU4U8BP711TR6KZ843/2CD0HDC5PS6A58T0P6E/compare?cellType=WholeTaxonomy&geneOption=CHRNA5&metadata=Cognitive%20Status&comparison=dotplot)  
230 [Taxonomy&geneOption=CHRNA5&metadata=Cognitive Status&comparison=dotplot.](https://knowledge.brain-map.org/data/5IU4U8BP711TR6KZ843/2CD0HDC5PS6A58T0P6E/compare?cellType=WholeTaxonomy&geneOption=CHRNA5&metadata=Cognitive%20Status&comparison=dotplot)) In the Human  
231 Protein Atlas database (brain single cell tissue) [https://www.proteinatlas.org/ENSG00000169684-](https://www.proteinatlas.org/ENSG00000169684-CHRNA5/single+cell+type/brain)  
232 [CHRNA5/single+cell+type/brain](https://www.proteinatlas.org/ENSG00000169684-CHRNA5/single+cell+type/brain), *CHRNA5* showed highest expression in a PVALB+ inhibitory cell type (c-  
233 41) which also showed highest expression of *SCUBE3* (Inhibitory neurons c-41, 15.1 normalized *CHRNA5*  
234 transcripts per million), likely also representing chandelier cells.

235 To investigate the cell type-specificity of the *CHRNA5* eQTL effects of the regulatory-SNP rs1979905 in  
236 the single nucleus data from ROS/MAP, we stratified the averaged *CHRNA5* expression by genotype for  
237 the rs1979905 A allele. We found that higher allelic dosage of the rs1979905 A allele was associated with  
238 greater *CHRNA5* expression (**Fig. 2C**), and that this pattern was most pronounced in subtypes of layer 5  
239 (L5 RORB IT:  $t = 2.460$ ,  $p = 0.0249$ ) and layer 6 (L6 IT THEMIS:  $t = 2.402$ ,  $p = 0.028$ ) excitatory neurons  
240 (**Fig. 2D**). In the stronger *CHRNA5*-expressing PVALB+ chandelier cells, however, the association did not  
241 reach significance. Other neuronal cell types appeared to diverge completely from the typical eQTL

242 pattern of rs1979905 (**Fig. 2C,D**). This analysis suggests that only a subset of cell-types contribute to the  
243 stepwise expression pattern observed in the prefrontal cortex by rs1979905 genotype.

244 Cell type specific data from ROS/MAP and the Allen database supports the hypothesis that *CHRNA5*  
245 possesses a distinctive expression pattern with enrichment in chandelier cell interneurons, compared to  
246 its more abundant and widely-expressed subunit partners.

#### 247 **Chandelier cells are significantly enriched for genes interacting with $\beta$ -amyloid**

248 To investigate the potential contribution of chandelier cells to  $\beta$ -amyloid processing, especially one that  
249 might be driven by nicotinic  $\alpha 5$ -containing receptors, we assessed the molecular function of genes which  
250 differentiate the chandelier cells from a different class of PVALB+ interneurons (basket cells). For this  
251 analysis we took advantage of a list of 222 such genes previously generated by Bakken and colleagues  
252 (30), who investigated the cellular identities of chandelier neurons in the cortex across species, including  
253 humans. Molecular functional pathway analysis revealed this list to be significantly enriched for genes  
254 defined as “amyloid-beta binding” (fold enrichment = 7.79,  $p(\text{FDR}) = 0.01$ ) (**Fig. 3A**), including *SORL1*, an  
255 endocytic receptor that directs the amyloid precursor protein away from the amyloidogenic pathway  
256 (45–47) and *EPHA4*, a receptor tyrosine kinase involved in amyloid regulation (48). Since  $\alpha 5$ -containing  
257 nicotinic receptors are highly permeable to calcium ions (21,22), we note that chandelier neurons are  
258 also significantly enriched for genes with a “calcium ion binding” molecular function (fold enrichment =  
259 3.77,  $p(\text{FDR}) = 4.12 \times 10^{-6}$ ) (**Fig. 3B**), including genes potentially protective against amyloid pathology such  
260 as *MME* and *SPOCK1*. Two genes are at the intersection of these functional pathways in chandelier cells,  
261 *PRNP* and *CLSTN2*. The former has been implicated in nicotinic receptor-mediated regulation of amyloid  
262 (49–52) and the latter is essential for normal cortical levels of GABAergic neurotransmission (53) These  
263 findings underscore the importance of investigating the relationship between the functional status of  
264 nicotinic  $\alpha 5$  subunits and chandelier neuron vulnerability to AD neuropathology.

#### 265 266 **A genotype-specific reduction in proportion of chandelier cells with increasing brain $\beta$ -amyloid levels**

267 To determine whether impaired function/trafficking  $\alpha 5$ -containing nicotinic receptors might promote  
268 chandelier neuron vulnerability to neurodegeneration, we examined the interaction of rs16969968  
269 genotype and AD neuropathology on estimated proportions of chandelier neurons in the bulk RNAseq  
270 dataset. This investigation was based on cell type proportion estimates for chandelier cells and several  
271 other interneuron subclasses, from sets of single-cell-informed marker genes, in a subset of 640  
272 ROS/MAP participants. Overall,  $\beta$ -amyloid levels were negatively associated with the proportion of  
273 chandelier cells ( $t = -4$ ,  $p = 7.26 \times 10^{-5}$ ). However, the missense rs16969968 A allele homozygotes showed  
274 significantly lower chandelier cell proportions with increasing  $\beta$ -amyloid load, compared to rs16969968 A  
275 allele non-carriers (interaction term  $t = -2.86$ ,  $p = 0.004$ )(**Fig. 4A,B,C**). In a secondary analysis, there is a  
276 suggestion of an opposite relationship of rs1979905 A allele and  $\beta$ -amyloid levels with chandelier cells  
277 but this does not reach statistical significance (interaction term  $t = 1.79$ ,  $p = 0.074$ )(**Fig. 4D,E,F**). The  
278 observed relationships between chandelier cell proportions, *CHRNA5* genotypes and amyloid were not  
279 altered by the inclusion of smoking status as a covariate in the analysis. Chandelier cell proportions did  
280 not correlate with tau pathology ( $t = -0.4$ ,  $p = 0.687$ ), nor was there an interaction of *CHRNA5* genotype  
281 and tau pathology with chandelier cell proportions (data not shown).

282 To assess whether the interaction between  $\beta$ -amyloid levels and *CHRNA5* SNPs was driven by the effects  
283 of these SNPs on *CHRNA5* expression, we assessed the effect of the interaction of *CHRNA5* levels and  $\beta$ -  
284 amyloid load on chandelier cell proportion but found no significant effect (interaction term,  $t = 0.5$ ,  $p =$   
285 0.619). This suggests that the genotype-specific association between amyloid load and chandelier cell



286 proportion is more likely driven by changes in nicotinic  $\alpha 5$  protein structure and/or trafficking (54) as a  
287 consequence of having two copies of the missense SNP in *CHRNA5*, rather than by the altered *CHRNA5*  
288 expression associated with the rs1979905 SNP genotype.

289 The schematic in **Fig. 5** illustrates a working model of the impact of the rs16969968 A allele  
290 homozygosity for chandelier cell vulnerability, as well as example mechanisms enriched in chandelier  
291 cells and known to alter  $\beta$ -amyloid processing.

292

## 293 **Discussion**

294 We examined human prefrontal cortical *CHRNA5* expression in aging, probing the connections between  
295 SNPs affecting the expression and function/trafficking of the nicotinic  $\alpha 5$  subunit gene and AD-related  
296 neuropathology. The aging prefrontal cortex demonstrates strong eQTL effects of the common  
297 regulatory-SNP rs1979905, and we show that the A allele of rs1979905 is associated with lower levels of  
298 brain  $\beta$ -amyloid. Single-nucleus RNAseq data revealed that chandelier cells have the greatest abundance  
299 of *CHRNA5* in human prefrontal cortex. These neurons are significantly enriched in amyloid-binding  
300 proteins, including some that may be activated via nicotinic receptors. Lastly, we examined the impact of  
301 AD neuropathology on the proportions of chandelier neurons and determined that the  $\alpha 5$ -altering  
302 common coding-SNP rs16969968 renders this interneuron population vulnerable to  $\beta$ -amyloid levels.  
303 Our findings, summarized in the working model in **Fig 5**, suggest a potential cell-type specific  
304 neuroprotective role for *CHRNA5* to reduce  $\beta$ -amyloid levels and toxicity.

## 305 **Inhibitory signalling is disrupted in Alzheimer's disease**

306 The disruption of the excitatory/inhibitory balance in the cortex is a hallmark of AD pathology and is  
307 associated with cognitive AD symptoms (3,4). Previous studies have shown disruption of cortical  
308 inhibitory signalling in AD stems from the alteration of the activity of inhibitory neurons and inhibitory  
309 cell loss (55–57). The susceptibility of inhibitory neurons to AD pathology is not uniform, however. While  
310 studies have shown significant drops in somatostatin-positive interneurons in the cortex of AD patients  
311 (58,59), the numbers of parvalbumin-positive cortical interneurons, including the PVALB+ chandelier  
312 cells, appear comparatively more resilient to AD pathology (59,60). Our study expands on these findings,  
313 demonstrating that the preservation of chandelier cells in AD pathology depends on the genotype of SNP  
314 in a nicotinic receptor subunit. The rs16969968 SNP is a missense mutation found to functionally alter  
315 the  $\alpha 5$ -containing nicotinic receptors in cell systems and *in vivo*, through altered channel biosynthesis,  
316 trafficking, properties and/or modulation (21,39,54,61,62). Recent optophysiological work suggests that  
317 the nicotinic  $\alpha 5$  subunit accelerates the endogenous cholinergic response in prefrontal cortex and  
318 protects it against desensitization (20), but little is known about endogenous cholinergic modulation of  
319 chandelier neurons.

## 320 **Chandelier cells are vulnerable to $\beta$ -amyloid pathology**

321 Chandelier cells are a specialized subtype of PVALB+ interneurons. They differ anatomically from the  
322 PVALB+ basket cells by their large number of vertically oriented axonal cartridges, which specifically  
323 innervate the axon initial segments of pyramidal neurons (63,64). New evidence suggests chandelier cells  
324 regulate excitation dynamics of neuronal networks (65). Impairment of these neurons has been  
325 implicated in diseases involving pathological excitation in the cortex, such as epilepsy (66,67) and AD  
326 (3,4,60). Our RNAseq findings are in agreement with previous work showing that the inhibitory output of

327 chandelier cells is sensitive to  $\beta$ -amyloid pathology (68) but unaffected by tau pathology (69). Chandelier  
328 cell axons near  $\beta$ -amyloid plaques have been found to show deformations, and pyramidal neurons  
329 proximal to plaques show loss of inhibitory input onto their axon initial segments (68). Our findings  
330 suggest that in people homozygous for A allele of the missense *CHRNA5* SNP rs16969968 (11% of the  
331 ROSMAP participants), this vulnerability of chandelier cells to  $\beta$ -amyloid pathology may be exacerbated,  
332 possibly leading to cell death.

### 333 **Potential mechanisms for a neuroprotective effect of $\alpha 5$ -containing nicotinic receptors**

334 Our results suggest that polymorphisms affecting *CHRNA5* expression and function, may alter both the  
335 total  $\beta$ -amyloid levels in the brain, and alter the susceptibility of specific *CHRNA5*-expressing cell types,  
336 such as the chandelier cells, to  $\beta$ -amyloid-mediated toxicity. One possible explanation for these  
337 observations may be the lowered binding of  $\beta$ -amyloid to the  $\alpha 4\beta 2\alpha 5$  nicotinic receptors (13) expressed  
338 by these cells. This protection against  $\beta$ -amyloid binding and inhibition of the nicotinic response (12)  
339 could promote resilience of nicotinic signalling in the chandelier cells, potentially leading to improved  
340 cell survival (14) in AD pathology. Furthermore, since  $\alpha 4\beta 2\alpha 5$  nicotinic receptors support higher  
341 conductance of calcium ions into the cell (21,22), another putative neuroprotective mechanism of the  $\alpha 5$   
342 subunit may be through driving possible calcium-dependent neuroprotective pathways in the neurons  
343 which express the  $\alpha 4\beta 2\alpha 5$  nicotinic receptors (70,71). Such calcium-regulated pathways may include  
344 *MME*, *SORL1*, *SPOCK1* or *PRNP*, which are specifically enriched in PVALB+ chandelier cells compared to  
345 PVALB+ non-chandelier cells (30), and which have been previously suggested to alter  $\beta$ -amyloid  
346 production and clearance (46,49,50,72).

### 347 **Caveats and opportunities for additional investigation**

348 While the ROS/MAP database offered an opportunity to assess the impact of *CHRNA5* expression and  
349 *CHRNA5*-related SNPs on AD pathology in a large sample, some caveats exist. As *CHRNA5* expression has  
350 previously been shown to be important for animal performance in demanding attentional tasks (23,24),  
351 one of the critical limitations of our study is that a robust attention assessment of the ROS/MAP  
352 individuals was not part of the study design, potentially explaining the lack of any association  
353 between *CHRNA5* expression or polymorphisms and a cognitive readout. While the ROS/MAP dataset  
354 presented an opportunity to study the effects of rs16969968 on a background of an unusually-low  
355 smoking prevalence (73), future work would benefit from more robust assessment of smoking history.

356 Although most prevalent in the prefrontal cortex, the  $\alpha 4\beta 2\alpha 5$  receptor is not the only type of  $\alpha 5$ -  
357 containing nicotinic receptor. Another type of interest is the  $\alpha 3\beta 4\alpha 5$  receptor, which is expressed  
358 primarily in the habenula (22), and intriguingly has all its subunits within the same locus (74).  
359 Unfortunately, expression data for the relevant *CHRNA3* and *CHRNB4* genes were not included in the  
360 prefrontal bulk RNAseq dataset, complicating investigation of hypotheses pertaining to the *CHRNA3*,  
361 *CHRNA5*, *CHRNB4* locus.  $\beta$ -amyloid pathology affects other types of nicotinic receptors besides the  
362  $\alpha 4\beta 2^*$  subtype, including the abundant and widely-expressed low-affinity homomeric  $\alpha 7$  receptor (10).  
363 However, since the activity and  $\beta$ -amyloid-sensitivity of the neuronal  $\alpha 4\beta 2^*$  receptor can be further  
364 modified by the inclusion of the auxiliary subunit  $\alpha 5$  (13), we focus on the high-affinity nicotinic receptor  
365 as a potentially rewarding target of study in the context of altered nicotinic signalling in AD.

366 A limitation of the single-nucleus RNA sequencing data (31) was its relatively low number of individuals,  
367 limiting the robustness of comparing the effects of rs1979905 on *CHRNA5* expression across the  
368 different cell types, and preventing a similar examination of cell-type specific effects of rs16969968

369 on *CHRNA5* expression in the ROSMAP dataset. This limitation should be considered when interpreting  
370 the findings of our study. Furthermore, the low numbers of individuals in the single-nucleus cohort also  
371 prevented a comparison between our findings from the estimated cell-type proportions in the bulk  
372 RNAseq data and the actual proportions of different cell types present in the single-nucleus data. Future  
373 studies involving more subjects with single-nucleus RNAseq data could extend our findings on the  
374 interaction association of the rs16969968 genotype and  $\beta$ -amyloid with chandelier cell proportions.

375 Since cortical cell-type proportions were estimated using patterns of marker gene expression (31), the  
376 decreased chandelier cell proportions may instead reflect reductions of chandelier cell cartridges in AD  
377 (60). While the disruption of cortical E/I balance would remain similar, a different interpretation of our  
378 data would be that the rs16969968 A allele homozygous genotype exacerbates chandelier cartridge loss  
379 and resulting in lower expression of chandelier-cell-specific marker genes in individuals with elevated  $\beta$ -  
380 amyloid.

381 Finally, while SNP exploration provides novel insight into the relationship between *CHRNA5* and  
382 neuropathology in aging, this work is limited by being correlational. Moreover, gene expression does not  
383 necessarily denote protein levels in AD brains (75) and thus differences in nicotinic receptor gene  
384 expression may not fully predict receptor levels or binding (76). Many questions remain about the  
385 mechanisms by which nicotinic receptors in chandelier cells regulate amyloid processing, as well as the  
386 consequences for this cell population when these mechanisms are disrupted. Work in model systems  
387 and larger snRNAseq datasets will be necessary to test specific hypotheses raised in this work.

### 388 **Summary and implications**

389 A growing body of work suggests that cortical excitability is perturbed early in Alzheimer's disease  
390 through impairment of inhibitory interneurons (55,77). *CHRNA5* is positioned to modulate the overall  
391 excitability of the prefrontal cortex in two ways: through the excitation of a population of deep layer  
392 cortical pyramidal neurons (20,78,79) that send projections throughout prefrontal cortex and, as  
393 ascertained from our findings in this study, through the excitation of specific subsets of cortical  
394 interneurons, the chandelier cells. Our findings suggest that *CHRNA5* is involved in Alzheimer's disease  
395 neuropathology. The A allele of the *CHRNA5* regulatory-SNP rs1979905 is associated with higher  
396 expression of *CHRNA5* and with reduced  $\beta$ -amyloid load in the brain. In parallel, the A allele of the  
397 missense SNP, rs16969968, is associated with fewer chandelier cells in individuals with high  $\beta$ -amyloid  
398 levels, suggesting that differences in the protein structure of *CHRNA5* contributes cellular resiliency to  $\beta$ -  
399 amyloid pathology. This combination suggests neuroprotective roles of *CHRNA5* in  $\beta$ -amyloid pathology  
400 and makes *CHRNA5* a target for therapies aiming to improve neuron survival in Alzheimer's disease.

401

402 **References**

- 403 1. Hampel H, Mesulam M-M, Cuello AC, Farlow MR, Giacobini E, Grossberg GT, et al. The cholinergic  
404 system in the pathophysiology and treatment of Alzheimer's disease. *Brain* [Internet]. 2018 Jul  
405 1;141(7):1917–33. Available from: <https://pubmed.ncbi.nlm.nih.gov/29850777>
- 406 2. Busche MA, Hyman BT. Synergy between amyloid- $\beta$  and tau in Alzheimer's disease. *Nat Neurosci*  
407 [Internet]. 2020;23(10):1183–93. Available from: <https://doi.org/10.1038/s41593-020-0687-6>
- 408 3. Lauterborn JC, Scaduto P, Cox CD, Schulmann A, Lynch G, Gall CM, et al. Increased excitatory to  
409 inhibitory synaptic ratio in parietal cortex samples from individuals with Alzheimer's disease. *Nat*  
410 *Commun* [Internet]. 2021;12(1):2603. Available from: [https://doi.org/10.1038/s41467-021-](https://doi.org/10.1038/s41467-021-22742-8)  
411 22742-8
- 412 4. Vico Varela E, Etter G, Williams S. Excitatory-inhibitory imbalance in Alzheimer's disease and  
413 therapeutic significance. *Neurobiol Dis* [Internet]. 2019;127:605–15. Available from:  
414 <https://www.sciencedirect.com/science/article/pii/S0969996118307599>
- 415 5. Pafundo DE, Miyamae T, Lewis DA, Gonzalez-Burgos G. Cholinergic  
416 modulation of neuronal excitability and recurrent excitation-inhibition in  
417 prefrontal cortex circuits: implications for gamma oscillations. *J Physiol*  
418 [Internet]. 2013/07/01. 2013 Oct 1;591(19):4725–48. Available from:  
419 <https://pubmed.ncbi.nlm.nih.gov/23818693>
- 420 6. Obermayer J, Luchicchi A, Heistek TS, de Kloet SF, Terra H, Bruinsma B, et al.  
421 Prefrontal cortical ChAT-VIP interneurons provide local excitation by cholinergic synaptic  
422 transmission and control attention. *Nat Commun* [Internet]. 2019;10(1):5280. Available from:  
423 <https://doi.org/10.1038/s41467-019-13244-9>
- 424 7. Bartus RT, Dean RL, Beer B, Lippa AS. The Cholinergic Hypothesis of Geriatric Memory  
425 Dysfunction. *Science* (80- ) [Internet]. 1982 Jul 30;217(4558):408–14. Available from:  
426 <https://doi.org/10.1126/science.7046051>
- 427 8. Court J, Martin-Ruiz C, Piggott M, Spurden D, Griffiths M, Perry E. Nicotinic receptor abnormalities  
428 in Alzheimer's disease. *Biol Psychiatry* [Internet]. 2001;49(3):175–84. Available from:  
429 <https://www.sciencedirect.com/science/article/pii/S0006322300011161>
- 430 9. Nordberg A, Winblad B. Reduced number of [3H]nicotine and [3H]acetylcholine binding sites in  
431 the frontal cortex of Alzheimer brains. *Neurosci Lett*. 1986 Dec;72(1):115–9.
- 432 10. Lasala M, Fabiani C, Corradi J, Antollini S, Bouzat C. Molecular Modulation of Human  $\alpha 7$  Nicotinic  
433 Receptor by Amyloid- $\beta$  Peptides. *Front Cell Neurosci* [Internet]. 2019;13. Available from:  
434 <https://www.frontiersin.org/article/10.3389/fncel.2019.00037>
- 435 11. Buckingham SD, Jones AK, Brown LA, Sattelle DB. Nicotinic acetylcholine receptor signalling: roles  
436 in Alzheimer's disease and amyloid neuroprotection. *Pharmacol Rev*. 2009 Mar;61(1):39–61.
- 437 12. Wu J, Kuo Y-P, George AA, Xu L, Hu J, Lukas RJ. beta-Amyloid directly inhibits human  $\alpha 4\beta 2$ -  
438 nicotinic acetylcholine receptors heterologously expressed in human SH-EP1 cells. *J Biol Chem*.  
439 2004 Sep;279(36):37842–51.
- 440 13. Lamb PW, Melton MA, Yakel JL. Inhibition of neuronal nicotinic acetylcholine receptor channels  
441 expressed in *Xenopus* oocytes by beta-amyloid1-42 peptide. *J Mol Neurosci*. 2005;27(1):13–21.
- 442 14. Kihara T, Shimohama S, Sawada H, Kimura J, Kume T, Kochiyama H, et al. Nicotinic receptor

- 443 stimulation protects neurons against beta-amyloid toxicity. *Ann Neurol*. 1997 Aug;42(2):159–63.
- 444 15. He N, Wang Z, Wang Y, Shen H, Yin M. ZY-1, A Novel Nicotinic Analog, Promotes Proliferation and  
445 Migration of Adult Hippocampal Neural Stem/Progenitor Cells. *Cell Mol Neurobiol* [Internet].  
446 2013;33(8):1149–57. Available from: <https://doi.org/10.1007/s10571-013-9981-0>
- 447 16. Nie H, Wang Z, Zhao W, Lu J, Zhang C, Lok K, et al. New nicotinic analogue ZY-1 enhances  
448 cognitive functions in a transgenic mice model of Alzheimer’s disease. *Neurosci Lett* [Internet].  
449 2013;537:29–34. Available from:  
450 <https://www.sciencedirect.com/science/article/pii/S0304394013000153>
- 451 17. Deardorff WJ, Feen E, Grossberg GT. The Use of Cholinesterase Inhibitors Across All Stages of  
452 Alzheimer’s Disease. *Drugs Aging* [Internet]. 2015;32(7):537–47. Available from:  
453 <https://doi.org/10.1007/s40266-015-0273-x>
- 454 18. Albuquerque EX, Pereira EFR, Alkondon M, Rogers SW. Mammalian Nicotinic Acetylcholine  
455 Receptors: From Structure to Function. *Physiol Rev* [Internet]. 2009;89(1):73–120. Available from:  
456 <https://doi.org/10.1152/physrev.00015.2008>
- 457 19. Ramirez-Latorre J, Yu CR, Qu X, Perin F, Karlin A, Role L. Functional contributions of  $\alpha 5$  subunit to  
458 neuronal acetylcholine receptor channels. *Nature* [Internet]. 1996;380(6572):347–51. Available  
459 from: <https://doi.org/10.1038/380347a0>
- 460 20. Venkatesan S, Lambe EK. Chrna5 is essential for a rapid and protected response to optogenetic  
461 release of endogenous acetylcholine in prefrontal cortex. *J Neurosci*. 2020;40(38).
- 462 21. Sciacaluga M, Monconi C, Martinello K, Catalano M, Bermudez I, Stitzel JA, et al. Crucial role of  
463 nicotinic  $\alpha 5$  subunit variants for  $Ca^{2+}$  fluxes in ventral midbrain neurons. *FASEB J* [Internet].  
464 2015;29(8):3389–98. Available from:  
465 <https://faseb.onlinelibrary.wiley.com/doi/abs/10.1096/fj.14-268102>
- 466 22. Scholze P, Huck S. The  $\alpha 5$  Nicotinic Acetylcholine Receptor Subunit Differentially Modulates  
467  $\alpha 4\beta 2^*$  and  $\alpha 3\beta 4^*$  Receptors. *Front Synaptic Neurosci* [Internet]. 2020;12. Available from:  
468 <https://www.frontiersin.org/article/10.3389/fnsyn.2020.607959>
- 469 23. Bailey CDC, De Biasi M, Fletcher PJ, Lambe EK. The Nicotinic Acetylcholine Receptor  $\alpha 5$  Subunit  
470 Plays a Key Role in Attention Circuitry and Accuracy. *J Neurosci* [Internet]. 2010 Jul 7;30(27):9241  
471 LP – 9252. Available from: <http://www.jneurosci.org/content/30/27/9241.abstract>
- 472 24. Howe WM, Brooks JL, Tierney PL, Pang J, Rossi A, Young D, et al.  $\alpha 5$  nAChR modulation of the  
473 prefrontal cortex makes attention resilient. *Brain Struct Funct*. 2018 Mar;223(2):1035–47.
- 474 25. Schuch JB, Polina ER, Rovaris DL, Kappel DB, Mota NR, Cupertino RB, et al. Pleiotropic effects of  
475 Chr15q25 nicotinic gene cluster and the relationship between smoking, cognition and ADHD. *J*  
476 *Psychiatr Res*. 2016 Sep;80:73–8.
- 477 26. Han W, Zhang T, Ni T, Zhu L, Liu D, Chen G, et al. Relationship of common variants in CHRNA5 with  
478 early-onset schizophrenia and executive function. *Schizophr Res*. 2019 Apr;206:407–12.
- 479 27. Jensen KP, DeVito EE, Herman AI, Valentine GW, Gelernter J, Sofuoglu M. A CHRNA5 Smoking Risk  
480 Variant Decreases the Aversive Effects of Nicotine in Humans. *Neuropsychopharmacology*  
481 [Internet]. 2015/05/07. 2015 Nov;40(12):2813–21. Available from:  
482 <https://pubmed.ncbi.nlm.nih.gov/25948103>
- 483 28. Livingston G, Huntley J, Sommerlad A, Ames D, Ballard C, Banerjee S, et al. Dementia prevention,

- 484 intervention, and care: 2020 report of the <em>Lancet</em> Commission. *Lancet* [Internet].  
485 2020 Aug 8;396(10248):413–46. Available from: [https://doi.org/10.1016/S0140-6736\(20\)30367-6](https://doi.org/10.1016/S0140-6736(20)30367-6)
- 486 29. Bennett DA, Buchman AS, Boyle PA, Barnes LL, Wilson RS, Schneider JA. Religious Orders Study  
487 and Rush Memory and Aging Project. *J Alzheimers Dis*. 2018;64(s1):S161–89.
- 488 30. Bakken TE, Jorstad NL, Hu Q, Lake BB, Tian W, Kalmbach BE, et al. Comparative cellular analysis of  
489 motor cortex in human, marmoset and mouse. *Nature* [Internet]. 2021;598(7879):111–9.  
490 Available from: <https://doi.org/10.1038/s41586-021-03465-8>
- 491 31. Cain A, Taga M, McCabe C, Hekselman I, White CC, Green G, et al. Multi-cellular communities are  
492 perturbed in the aging human brain and with alzheimer’s disease. *bioRxiv* [Internet]. 2020;  
493 Available from: <https://www.biorxiv.org/content/early/2020/12/23/2020.12.22.424084>
- 494 32. Ji X, Gui J, Han Y, Brennan P, Li Y, McKay J, et al. The role of haplotype in 15q25.1 locus in lung  
495 cancer risk: results of scanning chromosome 15. *Carcinogenesis*. 2015 Nov;36(11):1275–83.
- 496 33. Smith RM, Alachkar H, Papp AC, Wang D, Mash DC, Wang J-C, et al. Nicotinic  $\alpha 5$  receptor subunit  
497 mRNA expression is associated with distant 5’ upstream polymorphisms. *Eur J Hum Genet*  
498 [Internet]. 2011;19(1):76–83. Available from: <https://doi.org/10.1038/ejhg.2010.120>
- 499 34. Wessel J, McDonald SM, Hinds DA, Stokowski RP, Javitz HS, Kennemer M, et al. Resequencing of  
500 nicotinic acetylcholine receptor genes and association of common and rare variants with the  
501 Fagerström test for nicotine dependence. *Neuropsychopharmacology* [Internet]. 2010/08/25.  
502 2010 Nov;35(12):2392–402. Available from: <https://pubmed.ncbi.nlm.nih.gov/20736995>
- 503 35. Swan GE, Javitz HS, Jack LM, Wessel J, Michel M, Hinds DA, et al. Varenicline for smoking  
504 cessation: nausea severity and variation in nicotinic receptor genes. *Pharmacogenomics J*  
505 [Internet]. 2012;12(4):349–58. Available from: <https://doi.org/10.1038/tpj.2011.19>
- 506 36. Sadaghiani S, Ng B, Altmann A, Poline J-B, Banaschewski T, Bokde ALW, et al. Overdominant Effect  
507 of a CHRNA4 Polymorphism on Cingulo-Opercular Network Activity and Cognitive Control. *J*  
508 *Neurosci* [Internet]. 2017;37(40):9657–66. Available from:  
509 <https://www.jneurosci.org/content/37/40/9657>
- 510 37. De Jager PL, Ma Y, McCabe C, Xu J, Vardarajan BN, Felsky D, et al. A multi-omic atlas of the human  
511 frontal cortex for aging and Alzheimer’s disease research. *Sci Data* [Internet]. 2018;5(1):180142.  
512 Available from: <https://doi.org/10.1038/sdata.2018.142>
- 513 38. Satija R, Farrell JA, Gennert D, Schier AF, Regev A. Spatial reconstruction of single-cell gene  
514 expression data. *Nat Biotechnol* [Internet]. 2015;33(5):495–502. Available from:  
515 <https://doi.org/10.1038/nbt.3192>
- 516 39. Kuryatov A, Berrettini W, Lindstrom J. Acetylcholine receptor (AChR)  $\alpha 5$  subunit variant  
517 associated with risk for nicotine dependence and lung cancer reduces  $(\alpha 4\beta 2)_2\alpha 5$  AChR function.  
518 *Mol Pharmacol*. 2011 Jan;79(1):119–25.
- 519 40. Wang J-C, Spiegel N, Bertelsen S, Le N, McKenna N, Budde JP, et al. Cis-Regulatory Variants Affect  
520 CHRNA5 mRNA Expression in Populations of African and European Ancestry. *PLoS One* [Internet].  
521 2013 Nov 26;8(11):e80204. Available from: <https://doi.org/10.1371/journal.pone.0080204>
- 522 41. Hoft NR, Stitzel JA, Hutchison KE, Ehringer MA. CHRN2 promoter region: association with  
523 subjective effects to nicotine and gene expression differences. *Genes Brain Behav* [Internet].  
524 2010/11/04. 2011 Mar;10(2):176–85. Available from: <https://pubmed.ncbi.nlm.nih.gov/20854418>

- 525 42. Jensen KP, Devito EE, Herman AI, Valentine GW, Gelernter J, Sofuoglu M. A CHRNA5 smoking risk  
526 variant decreases the aversive effects of nicotine in humans. *Neuropsychopharmacology*.  
527 2015;40(12):2813–21.
- 528 43. Benjamini Y, Hochberg Y. Controlling the False Discovery Rate: A Practical and Powerful Approach  
529 to Multiple Testing. *J R Stat Soc Ser B [Internet]*. 1995 Jan 26;57(1):289–300. Available from:  
530 <http://www.jstor.org/stable/2346101>
- 531 44. Hodge RD, Bakken TE, Miller JA, Smith KA, Barkan ER, Graybuck LT, et al. Conserved cell types  
532 with divergent features in human versus mouse cortex. *Nature*. 2019 Sep;573(7772):61–8.
- 533 45. Andersen OM, Reiche J, Schmidt V, Gotthardt M, Spoelgen R, Behlke J, et al. Neuronal sorting  
534 protein-related receptor sorLA/LR11 regulates processing of the amyloid precursor protein. *Proc*  
535 *Natl Acad Sci [Internet]*. 2005;102(38):13461–6. Available from:  
536 <https://www.pnas.org/doi/abs/10.1073/pnas.0503689102>
- 537 46. Caglayan S, Takagi-Niidome S, Liao F, Carlo A-S, Schmidt V, Burgert T, et al. Lysosomal Sorting of  
538 Amyloid- $\beta$  by the SORLA Receptor Is Impaired by a Familial Alzheimer’s Disease Mutation. *Sci*  
539 *Transl Med [Internet]*. 2014;6(223):223ra20–223ra20. Available from:  
540 <https://www.science.org/doi/abs/10.1126/scitranslmed.3007747>
- 541 47. Hung C, Tuck E, Stubbs V, van der Lee SJ, Aalfs C, van Spaendonk R, et al. SORL1 deficiency in  
542 human excitatory neurons causes APP-dependent defects in the endolysosome-autophagy  
543 network. *Cell Rep [Internet]*. 2021;35(11):109259. Available from:  
544 <https://www.sciencedirect.com/science/article/pii/S2211124721006239>
- 545 48. Tamura K, Chiu Y-W, Shiohara A, Hori Y, Tomita T. EphA4 regulates A $\beta$  production via BACE1  
546 expression in neurons. *FASEB J Off Publ Fed Am Soc Exp Biol*. 2020 Dec;34(12):16383–96.
- 547 49. Griffiths HH, Whitehouse IJ, Hooper NM. Regulation of amyloid- $\beta$  production by the prion protein.  
548 *Prion [Internet]*. 2012/07/01. 2012 Jul 1;6(3):217–22. Available from:  
549 <https://pubmed.ncbi.nlm.nih.gov/22449984>
- 550 50. Nie H, Li Z, Lukas RJ, Shen Y, Song L, Wang X, et al. Construction of SH-EP1-alpha4beta2-hAPP695  
551 cell line and effects of nicotinic agonists on beta-amyloid in the cells. *Cell Mol Neurobiol*. 2008  
552 Jan;28(1):103–12.
- 553 51. Beraldo FH, Arantes CP, Santos TG, Queiroz NGT, Young K, Rylett RJ, et al. Role of alpha7 nicotinic  
554 acetylcholine receptor in calcium signaling induced by prion protein interaction with stress-  
555 inducible protein 1. *J Biol Chem*. 2010 Nov;285(47):36542–50.
- 556 52. Nygaard HB, Strittmatter SM. Cellular Prion Protein Mediates the Toxicity of  $\beta$ -Amyloid  
557 Oligomers: Implications for Alzheimer Disease. *Arch Neurol [Internet]*. 2009;66(11):1325–8.  
558 Available from: <https://doi.org/10.1001/archneurol.2009.223>
- 559 53. Lipina T V, Prasad T, Yokomaku D, Luo L, Connor SA, Kawabe H, et al. Cognitive Deficits in  
560 Calsyntenin-2-deficient Mice Associated with Reduced GABAergic Transmission.  
561 *Neuropsychopharmacol Off Publ Am Coll Neuropsychopharmacol*. 2016 Feb;41(3):802–10.
- 562 54. Maskos U. The nicotinic receptor alpha5 coding polymorphism rs16969968 as a major target in  
563 disease: Functional dissection and remaining challenges. *J Neurochem [Internet]*.  
564 2020;154(3):241–50. Available from: <https://onlinelibrary.wiley.com/doi/abs/10.1111/jnc.14989>
- 565 55. Hijazi S, Heistek TS, Scheltens P, Neumann U, Shimshek DR, Mansvelder HD, et al. Early

- 566 restoration of parvalbumin interneuron activity prevents memory loss and network  
567 hyperexcitability in a mouse model of Alzheimer’s disease. *Mol Psychiatry* [Internet].  
568 2020;25(12):3380–98. Available from: <https://doi.org/10.1038/s41380-019-0483-4>
- 569 56. Wright AL, Zinn R, Hohensinn B, Konen LM, Beynon SB, Tan RP, et al. Neuroinflammation and  
570 neuronal loss precede A $\beta$  plaque deposition in the hAPP-J20 mouse model of Alzheimer’s  
571 disease. *PLoS One*. 2013;8(4):e59586.
- 572 57. Zheng J, Li H-L, Tian N, Liu F, Wang L, Yin Y, et al. Interneuron Accumulation of Phosphorylated tau  
573 Impairs Adult Hippocampal Neurogenesis by Suppressing GABAergic Transmission. *Cell Stem Cell*  
574 [Internet]. 2020 Mar 5;26(3):331-345.e6. Available from:  
575 <https://doi.org/10.1016/j.stem.2019.12.015>
- 576 58. Beal MF, Mazurek MF, Svendsen CN, Bird ED, Martin JB. Widespread reduction of somatostatin-  
577 like immunoreactivity in the cerebral cortex in Alzheimer’s disease. *Ann Neurol*. 1986  
578 Oct;20(4):489–95.
- 579 59. Waller R, Mandeya M, Viney E, Simpson JE, Wharton SB. Histological characterization of  
580 interneurons in Alzheimer’s disease reveals a loss of somatostatin interneurons in the temporal  
581 cortex. *Neuropathology*. 2020 Aug;40(4):336–46.
- 582 60. Fonseca M, Soriano E, Ferrer I, Martinez A, Tun~on T, Chandelier cell axons identified by  
583 parvalbumin-immunoreactivity in the normal human temporal cortex and in Alzheimer’s disease.  
584 *Neuroscience* [Internet]. 1993;55(4):1107–16. Available from:  
585 <https://www.sciencedirect.com/science/article/pii/0306452293903249>
- 586 61. Koukouli F, Rooy M, Tziotis D, Sailor KA, O’Neill HC, Levenga J, et al. Nicotine reverses  
587 hypofrontality in animal models of addiction and schizophrenia. *Nat Med* [Internet].  
588 2017;23(3):347–54. Available from: <https://doi.org/10.1038/nm.4274>
- 589 62. Forget B, Scholze P, Langa F, Morel C, Pons S, Mondoloni S, et al. A Human Polymorphism in  
590 CHRNA5 Is Linked to Relapse to Nicotine Seeking in Transgenic Rats. *Curr Biol* [Internet].  
591 2018;28(20):3244-3253.e7. Available from:  
592 <https://www.sciencedirect.com/science/article/pii/S096098221831128X>
- 593 63. Fairén A, Valverde F. A specialized type of neuron in the visual cortex of cat: a Golgi and electron  
594 microscope study of chandelier cells. *J Comp Neurol*. 1980 Dec;194(4):761–79.
- 595 64. Somogyi P. A specific “axo-axonal” interneuron in the visual cortex of the rat. *Brain Res*. 1977  
596 Nov;136(2):345–50.
- 597 65. Schneider-Mizell CM, Bodor AL, Collman F, Brittain D, Bleckert A, Dorkenwald S, et al. Structure  
598 and function of axo-axonic inhibition. Calabrese RL, Callaway E, Huang ZJ, Oberlaender M, editors.  
599 *Elife* [Internet]. 2021;10:e73783. Available from: <https://doi.org/10.7554/eLife.73783>
- 600 66. Ribak CE. Axon terminals of GABAergic chandelier cells are lost at epileptic foci. *Brain Res*  
601 [Internet]. 1985;326(2):251–60. Available from:  
602 <https://www.sciencedirect.com/science/article/pii/0006899385900344>
- 603 67. Zhu Y, Stornetta RL, Zhu JJ. Chandelier Cells Control Excessive Cortical Excitation: Characteristics  
604 of Whisker-Evoked Synaptic Responses of Layer 2/3 Nonpyramidal and Pyramidal Neurons. *J*  
605 *Neurosci* [Internet]. 2004 Jun 2;24(22):5101 LP – 5108. Available from:  
606 <http://www.jneurosci.org/content/24/22/5101.abstract>



- 607 68. León-Espinosa G, DeFelipe J, Muñoz A. Effects of amyloid- $\beta$  plaque proximity on the axon initial  
608 segment of pyramidal cells. *J Alzheimers Dis.* 2012;29(4):841–52.
- 609 69. Blazquez-Llorca L, Garcia-Marin V, Defelipe J. Pericellular innervation of neurons expressing  
610 abnormally hyperphosphorylated tau in the hippocampal formation of Alzheimer's disease  
611 patients. *Front Neuroanat.* 2010;4:20.
- 612 70. Ueda M, Iida Y, Kitamura Y, Kawashima H, Ogawa M, Magata Y, et al. 5-Iodo-A-85380, a specific  
613 ligand for alpha 4 beta 2 nicotinic acetylcholine receptors, prevents glutamate neurotoxicity in  
614 rat cortical cultured neurons. *Brain Res.* 2008 Mar;1199:46–52.
- 615 71. Cingir Koker S, Jahja E, Shehwana H, Keskus AG, Konu O. Cholinergic Receptor Nicotinic Alpha 5  
616 (CHRNA5) RNAi is associated with cell cycle inhibition, apoptosis, DNA damage response and drug  
617 sensitivity in breast cancer. *PLoS One.* 2018;13(12):e0208982.
- 618 72. Barrera-Ocampo A, Arlt S, Matschke J, Hartmann U, Puig B, Ferrer I, et al. Amyloid- $\beta$  Precursor  
619 Protein Modulates the Sorting of Testican-1 and Contributes to Its Accumulation in Brain Tissue  
620 and Cerebrospinal Fluid from Patients with Alzheimer Disease. *J Neuropathol Exp Neurol*  
621 [Internet]. 2016 Sep 1;75(9):903–16. Available from: <https://doi.org/10.1093/jnen/nlw065>
- 622 73. Cornelius ME, Loretan CG, Wang TW, Jamal A, Moma DM. Tobacco Product Use Among Adults —  
623 United States, 2020. *MMWR Morb Mortal Wkly Rep.* 2022;71:397–405.
- 624 74. Bierut LJ, Stitzel JA, Wang JC, Hinrichs AL, Grucza RA, Xuei X, et al. Variants in nicotinic receptors  
625 and risk for nicotine dependence. *Am J Psychiatry* [Internet]. 2008/06/02. 2008 Sep;165(9):1163–  
626 71. Available from: <https://pubmed.ncbi.nlm.nih.gov/18519524>
- 627 75. Johnson ECB, Carter EK, Dammer EB, Duong DM, Gerasimov ES, Liu Y, et al. Large-scale deep  
628 multi-layer analysis of Alzheimer's disease brain reveals strong proteomic disease-related changes  
629 not observed at the RNA level. *Nat Neurosci* [Internet]. 2022;25(2):213–25. Available from:  
630 <https://doi.org/10.1038/s41593-021-00999-y>
- 631 76. Hansen JY, Markello RD, Tuominen L, Nørgaard M, Kuzmin E, Palomero-Gallagher N, et al.  
632 Correspondence between gene expression and neurotransmitter receptor and transporter  
633 density in the human brain. *Neuroimage* [Internet]. 2022;264:119671. Available from:  
634 <https://www.sciencedirect.com/science/article/pii/S1053811922007923>
- 635 77. Petrache AL, Rajulawalla A, Shi A, Wetzel A, Saito T, Saido TC, et al. Aberrant Excitatory-Inhibitory  
636 Synaptic Mechanisms in Entorhinal Cortex Microcircuits During the Pathogenesis of Alzheimer's  
637 Disease. *Cereb Cortex* [Internet]. 2019 Apr 1;29(4):1834–50. Available from:  
638 <https://pubmed.ncbi.nlm.nih.gov/30766992>
- 639 78. Wada E, McKinnon D, Heinemann S, Patrick J, Swanson LW. The distribution of mRNA encoded by  
640 a new member of the neuronal nicotinic acetylcholine receptor gene family (alpha 5) in the rat  
641 central nervous system. *Brain Res.* 1990 Aug;526(1):45–53.
- 642 79. Winzer-Serhan UH, Leslie FM. Expression of alpha5 nicotinic acetylcholine receptor subunit mRNA  
643 during hippocampal and cortical development. *J Comp Neurol.* 2005 Jan;481(1):19–30.
- 644
- 645

646 **Figure legends**

647 **Figure 1. SNPs affecting expression of  $\alpha 4\beta 2^*$  nicotinic receptor subunit genes highlight a link between**  
648 ***CHRNA5* and amyloid pathology. A,** Schematics illustrating different subunit compositions of prefrontal  
649  $\alpha 4\beta 2^*$  nicotinic receptors, with and without the  $\alpha 5$  subunit. **B,** Localization of the rs16969968 and  
650 rs1979905 SNPs in relation to the *CHRNA5* locus. **C,** The A allele of the missense SNP rs16969968 (left) in  
651 the coding region of *CHRNA5* is associated with lowered *CHRNA5* expression, while the A allele of the  
652 rs1979905 SNP (middle) upstream of the *CHRNA5* gene is associated with enhanced *CHRNA5* expression.  
653 Data from the DLPFC of ROS/MAP individuals. **D,** *CHRNA5* expression appears to be controlled by the  
654 zygosity of the rs1979905 A allele (colors) instead of the rs16969968 A allele (x-axis). Data shown as  
655 *CHRNA5* expression for each subject with means indicated. **E,** eQTL effects of SNPs in nicotinic subunit  
656 genes on their respective gene expression. Shown as  $\beta$ -coefficient with significance (p) in brackets. **F,**  
657 Network plot depicting the relationships between SNPs (black), gene expression (red), neuropathology  
658 (blue), and last global cognition score (green). Solid and dashed lines indicate whether association was  
659 significant after correction for FDR or not, respectively. **G,** Network plot depicting the correlations  
660 present between the expression of select cholinergic genes in the DLPFC. Colour of lines indicates  
661 direction of correlation (negative or positive) while the thickness indicates correlation strength. All  
662 correlations shown are significant after adjustment for FDR.

663 **Figure 2. *CHRNA5* expression is elevated in chandelier cells and is affected by genotype for the**  
664 **rs1979905 A allele. A,** Expression of *CHRNA5* averaged per cell type per individual, original gene count  
665 values were normalized for each cell by total expression. F-test significance of ANOVA shown on graph,  
666 with red asterisk denoting post-hoc tests demonstrating *CHRNA5* expression is stronger in chandelier  
667 cells compared to all but one other cell type. Mean expression of *CHRNA5* in chandelier cells displayed  
668 (red line). **B,** Expression of *CHRNA4* (left) and *CHRN2* (right) across different cell types in the ROS/MAP  
669 DLPFC snRNAseq dataset. Mean expression of *CHRNA4* or *CHRN2* in chandelier cells displayed (red line).  
670 Data shown as mean + SEM of the data averaged per cell-type per individual. **C,** Expression of *CHRNA5*  
671 across cell types in the PFC in individuals split by genotype for the rs1979905 A allele, expression  
672 averaged per cell type per individual. Number of individuals per rs1979905 A allele genotype: 0, n = 5; 1,  
673 n = 13; 2, n = 4. **D,** Effect of genotype for rs1979905 A allele on expression of *CHRNA5* in selected cell  
674 types, data shown as *CHRNA5* expression averaged per cell type per individual. A pattern of increasing  
675 *CHRNA5* expression with increasing rs1979905 A zygosity is present in some cell types. Significance  
676 shown for linear regression models for L5 and L6 excitatory neurons. Displayed as mean + SEM. Number  
677 of cells per subtype indicated ( $n_{\text{cell}}$ ).

678 **Figure 3. Chandelier cells are significantly enriched for genes interacting with amyloid. A,** Ontology  
679 (molecular function) of gene set upregulated in cortical PVALB+ chandelier cells vs. PVALB+ non-  
680 chandelier cells. Only molecular functions with significant fold enrichment after FDR are displayed.  
681 “Calcium ion-binding” and “amyloid-beta binding” functions are highlighted. **B,** Venn diagram displaying  
682 genes from **A** with either a “calcium ion-binding” or a “amyloid-beta binding” molecular function, and  
683 their overlap.

684 **Figure 4. Association of chandelier cell proportions with  $\beta$ -amyloid load is dependent on the**  
685 **rs16969968 A allele genotype.** Cell type proportion data for interneuron populations is available for  
686 almost a third of the deceased ROS/MAP subjects, allowing the assessment of the interaction among  
687 chandelier cell proportion, brain amyloid load, and the *CHRNA5* SNP haplotype. **A,B** Stratifying by  
688 rs16969968 A allele reveals a significant interaction effect between rs16969968 A allele and amyloid load

689 on chandelier cell proportions with rs16969968 A allele homozygotes showing a more negative  
690 association between brain amyloid load and chandelier cell proportions compared to rs16969968 A allele  
691 non-carriers (interaction term  $t = -2.86$ ,  $p = 0.004$ ). Scatter plots show 95% confidence intervals of linear  
692 model predictions,  $\beta$ -coefficients and  $p$  values of individual linear regression models are displayed. **C**,  
693 Overlay of the linear models from A,B, showing 95% confidence intervals. **D,E**, Stratifying by rs1979905  
694 A allele shows a suggestion of an opposite interaction between rs1979905 A allele and amyloid load on  
695 chandelier cell proportions (interaction term  $t = 1.769$ ,  $p = 0.078$ ). Scatter plots show 95% confidence  
696 intervals of linear model predictions,  $\beta$ -coefficients and  $p$  values of individual linear regression models  
697 are displayed. **F**, Overlay of the linear models from D,E, showing 95% confidence intervals.

698  
699 **Figure 5. A working model of the potential role of chandelier cells in  $\beta$ -amyloid processing, and of the**

700 **impact of *CHRNA5* genotype on chandelier cell (ChC) resilience and vulnerability.** Top: Chandelier cells  
701 are significantly enriched for multiple genes involved in  $\beta$ -amyloid processing and degradation including  
702 for example neprilysin (NEP), a potentially *CHRNA5*-regulated degrader of  $\beta$ -amyloid, and SORL1, a vital  
703 component of the APP-recycling pathway. Bottom: In coding-SNP rs16969968 non-carriers, the  $\alpha 4\beta 2\alpha 5$   
704 nicotinic receptor is resistant to inhibition by  $\beta$ -amyloid, preserving nicotinic signalling even at high  $\beta$ -  
705 amyloid levels that inhibit the  $\alpha 4\beta 2$  receptors. In coding-SNP rs16969968 homozygous individuals, the  
706 disruption of the  $\alpha 5$  subunit may reduce its representation in the receptors or block its protective  
707 function against  $\beta$ -amyloid, leading to disrupted nicotinic signalling at higher  $\beta$ -amyloid levels, possibly  
708 triggering a cytotoxic response in the chandelier cells.

709

710

711 **Table 1.** Expression correlation of selected cholinergic genes. Results of Pearson's correlation analysis of  
712 the expression of selected cholinergic genes using the bulk tissue RNAseq data from the DLPFC of  
713 ROS/MAP subjects.

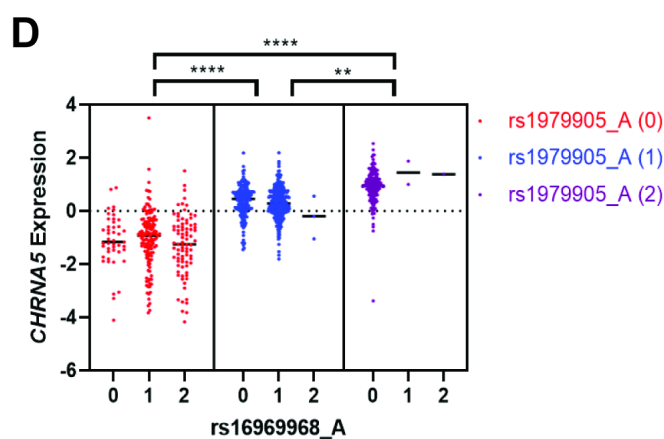
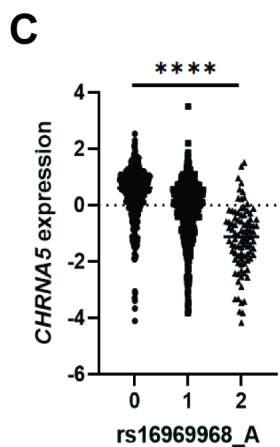
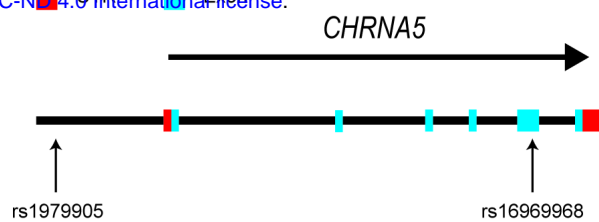
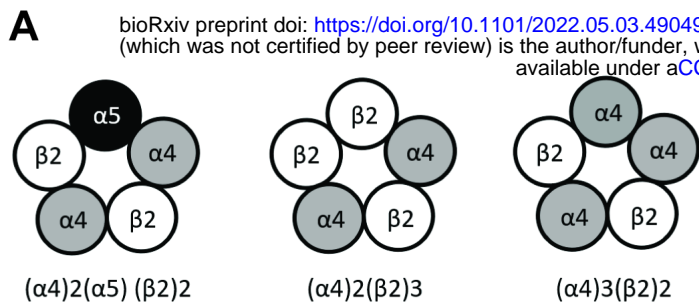
714

715

716

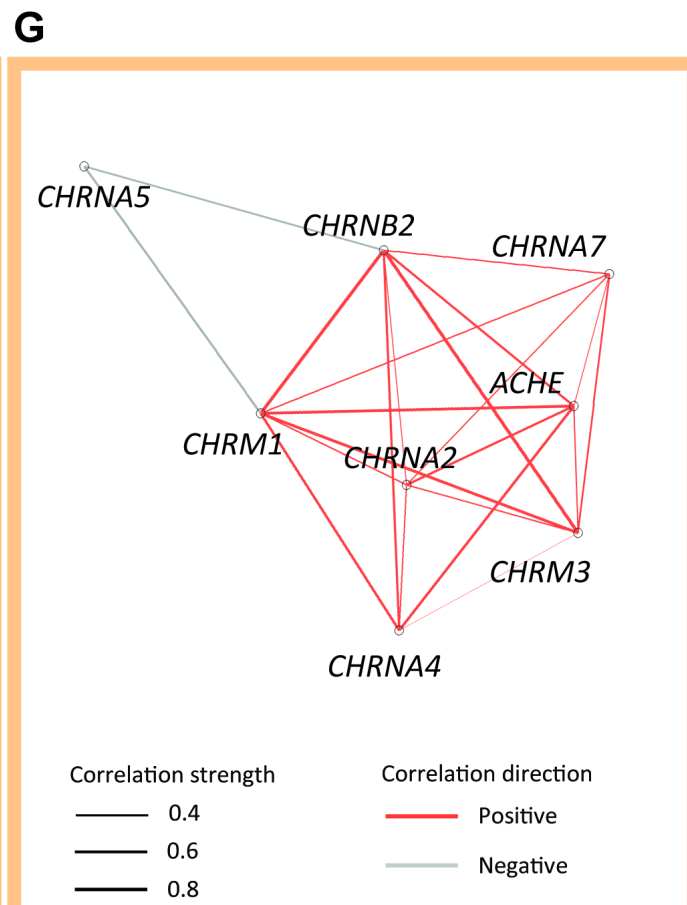
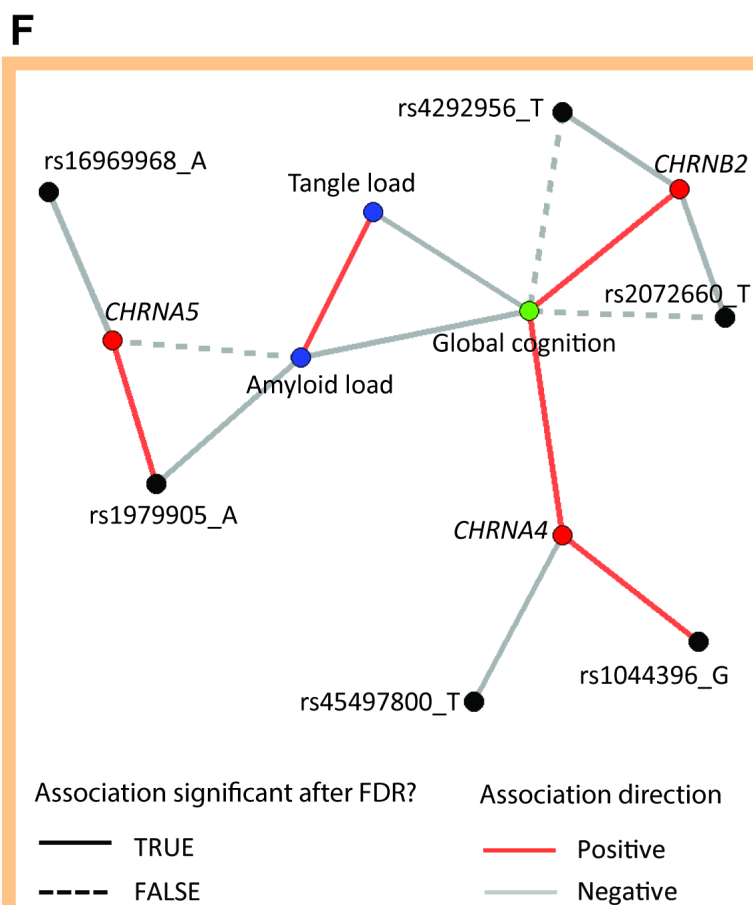
717

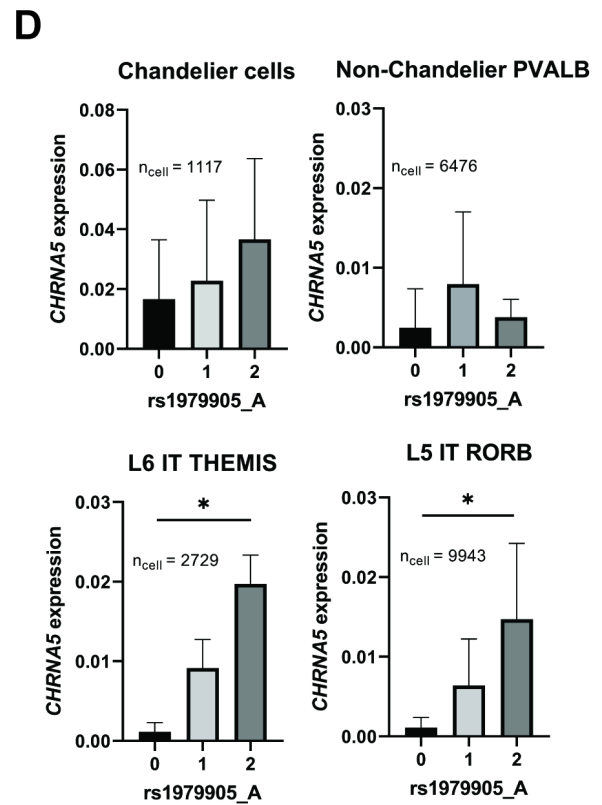
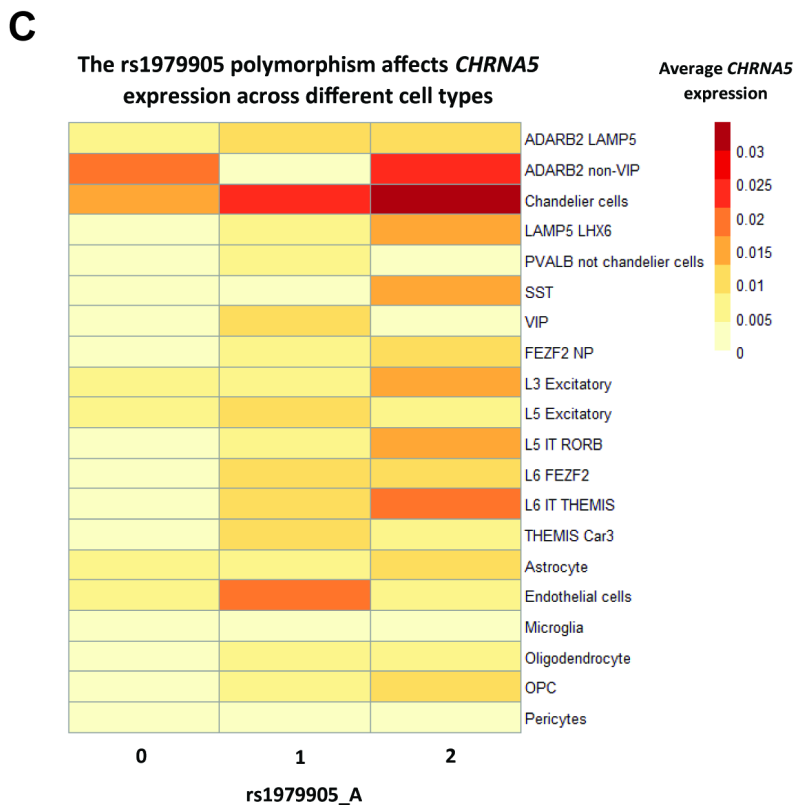
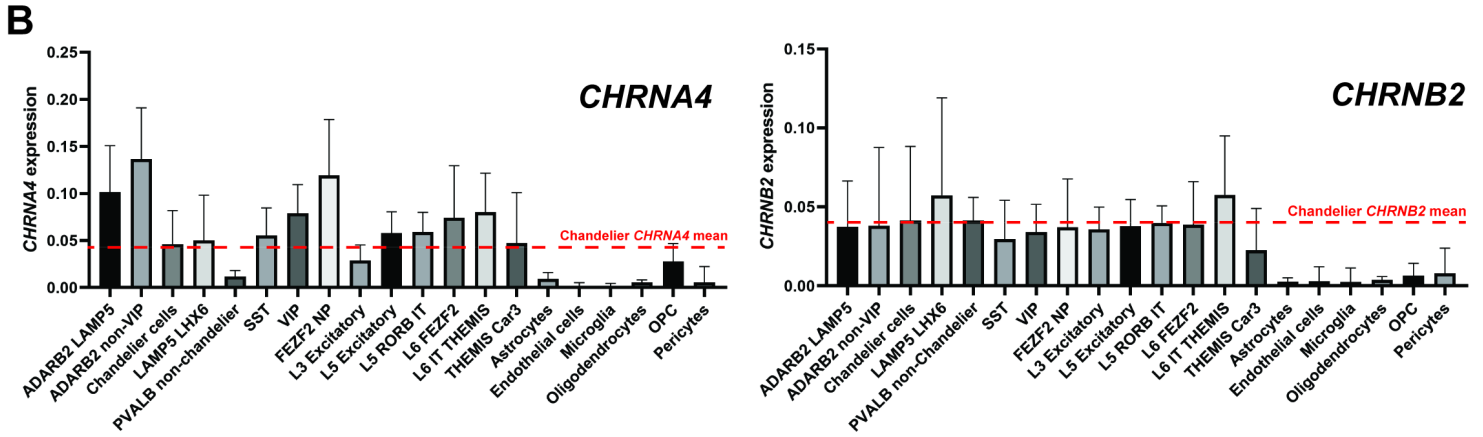
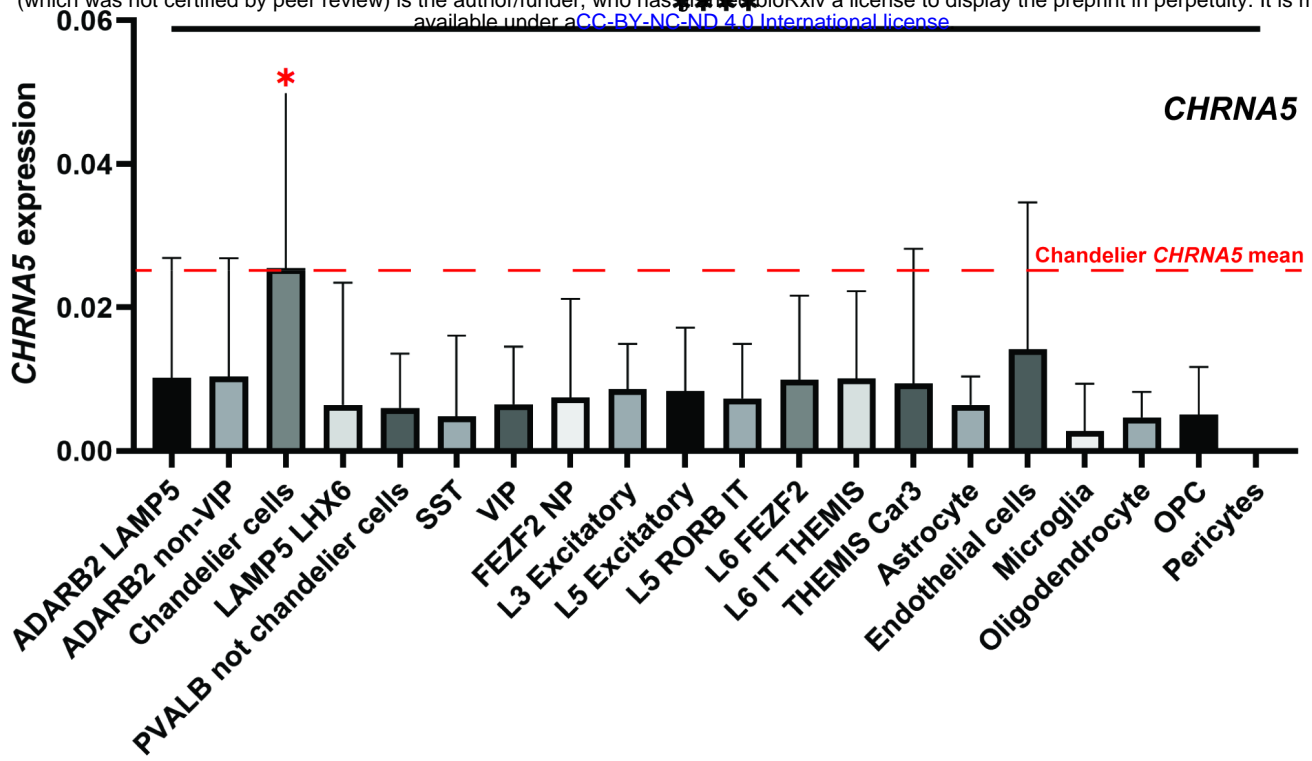
<b>Gene 1</b>	<b>Gene 2</b>	<b>r</b>	<b>p</b>	<b>FDR</b>
<i>CHRNA4</i>	<i>ACHE</i>	0.556	<0.001	<0.001
	<i>CHRM1</i>	0.542	<0.001	<0.001
	<i>CHRM3</i>	0.242	<0.001	0.002
	<i>CHRNA2</i>	0.307	<0.001	<0.001
	<i>CHRNA7</i>	0.131	0.039	0.464
	<i>CHRNB2</i>	0.457	<0.001	<0.001
<i>CHRNA5</i>	<i>ACHE</i>	0.063	0.324	1.000
	<i>CHRM1</i>	-0.309	<0.001	<0.001
	<i>CHRM3</i>	-0.095	0.134	1.000
	<i>CHRNA2</i>	-0.045	0.477	1.000
	<i>CHRNA4</i>	-0.130	0.041	0.464
	<i>CHRNA7</i>	-0.061	0.342	1.000
	<i>CHRNB2</i>	-0.248	<0.001	0.001
<i>CHRNB2</i>	<i>ACHE</i>	0.472	<0.001	<0.001
	<i>CHRM1</i>	0.846	<0.001	<0.001
	<i>CHRM3</i>	0.645	<0.001	<0.001
	<i>CHRNA2</i>	0.283	<0.001	<0.001
	<i>CHRNA4</i>	0.457	<0.001	<0.001
	<i>CHRNA7</i>	0.359	<0.001	<0.001



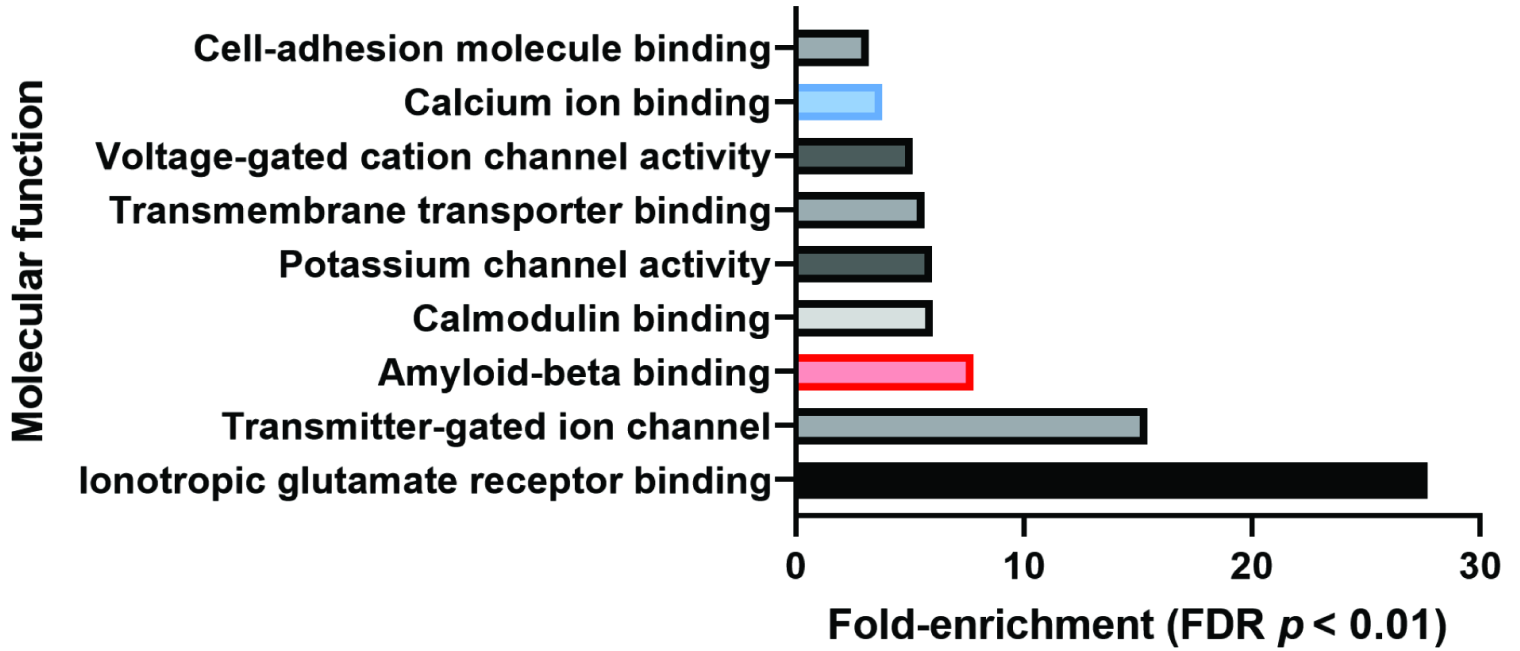
**E**

SNP/Gene	<i>CHRNA5</i>	<i>CHRNA4</i>	<i>CHRNA2</i>
rs1979905_A	1.083 ( $5.94 \times 10^{-124}$ )	-	-
rs16969968_A	-0.713 ( $3.98 \times 10^{-40}$ )	-	-
rs1044396_G	-	0.075 (0.0003)	-
rs4549700_T	-	-0.181 ( $1.32 \times 10^{-11}$ )	-
rs4292956_T	-	-	-0.209 ( $2.02 \times 10^{-7}$ )
rs2072660_T	-	-	-0.128 ( $7.05 \times 10^{-7}$ )





## Ontology of genes upregulated in chandelier vs. basket cells



**B**

